Title
A Guide to Studying Human Hair Follicle Cycling In Vivo

Journal
JOURNAL OF INVESTIGATIVE DERMATOLOGY, 136(1)

ISSN
0022-202X

Authors
Oh, Ji Won
Kloepper, Jennifer
Langan, Ewan A
et al.

Publication Date
2016

DOI
10.1038/JID.2015.354

Peer reviewed

HHS Public Access

Author manuscript

J Invest Dermatol. Author manuscript; available in PMC 2016 July 01.

Published in final edited form as:

J Invest Dermatol. 2016 January ; 136(1): 34–44. doi:10.1038/JID.2015.354.

A guide to studying human hair follicle cycling *in vivo*

Ji Won Oh[1,2,3,4,5], **Jennifer Kloepper**[6], **Ewan A. Langan**[6], **Yongsoo Kim**[7], **Joongyeub Yeo**[8], **Min Ji Kim**[9], **Tsai-Ching Hsi**[3,4,5], **Christian Rose**[10], **Ghil Suk Yoon**[11], **Seok-Jong Lee**[9], **John Seykora**[12], **Jung Chul Kim**[1,2], **Young Kwan Sung**[2], **Moonkyu Kim**[#1,2,#], **Ralf Paus**[#13,14,#], and **Maksim V. Plikus**[#3,4,5,#]

[1]Hair Transplantation Center, Kyungpook National University Hospital, Daegu, Korea [2]Department of Immunology, School of Medicine, Kyungpook National University, Daegu, Korea [3]Department of Developmental and Cell Biology, University of California, Irvine, Irvine, CA 92697, USA [4]Sue and Bill Gross Stem Cell Research Center, University of California, Irvine, Irvine, CA 92697, USA [5]Center for Complex Biological Systems, University of California, Irvine, Irvine, CA 92697, USA [6]Department of Dermatology, University of Lübeck, Lübeck, Germany [7]Division of Molecular Pathology, the Netherlands Cancer Institute, Amsterdam, the Netherlands [8]Institute for Computational and Mathematical Engineering, Stanford University, Stanford, CA 94305, USA [9]Department of Dermatology, Kyungpook National University School of Medicine, Daegu, Korea [10]Dermatohistologisches Labor Rose/Bartsch, Luebeck, Germany [11]Departments of Pathology, Kyungpook National University School of Medicine, Daegu, Korea [12]Department of Dermatology, University of Pennsylvania, Philadelphia, PA 19104, USA [13]Dermatology Research Centre, Institute of Inflammation and Repair, University of Manchester, Manchester, M13 9PL, UK [14]Department of Dermatology, University of Münster, Münster, Germany

[#] These authors contributed equally to this work.

Abstract

Hair follicles (HFs) undergo life-long cyclical transformations, progressing through stages of rapid growth (anagen), regression (catagen), and relative “quiescence” (telogen). Since HF cycling abnormalities underlie many human hair growth disorders, the accurate classification of individual cycle stages within skin biopsies is clinically important and essential for hair research. For preclinical human hair research purposes, human scalp skin can be xenografted onto immunocompromised mice to study human HF cycling and manipulate long-lasting anagen *in vivo*. While available for mice, a comprehensive guide on how to recognize different human hair cycle stages *in vivo* is lacking. Here, we present such a guide, which uses objective, well-defined, and reproducible criteria and integrates simple morphological indicators with advanced, (immuno)-histochemical markers. This guide also characterizes human HF cycling in xenografts

[#] Authors for correspondence: Moonkyu Kim, Department of Immunology, School of Medicine, Kyungpook National University, Daegu, Korea. moonkim@knu.ac.kr, Ralf Paus, Dermatology Research Centre, Institute of Inflammation and Repair, University of Manchester, Manchester, M13 9PL, UK. ralf.paus@manchester.ac.uk, Maksim V. Plikus, Department of Developmental and Cell Biology, University of California Irvine, Irvine, California 92697, USA. plikus@uci.edu.

Conflict of Interest The authors state no conflict of interest.

and highlights the utility of this model for *in vivo* hair research. Detailed schematic drawings and representative micrographs provide examples of how best to identify human HF stages, even in sub-optimally sectioned tissue, and practical recommendations are given for designing human-on-mouse hair cycle experiments. Thus, this guide seeks to offer a benchmark for human hair cycle stage classification, for both hair research experts and newcomers to the field.

Introduction

Limitations of the murine hair follicle model

Human and murine hair follicles (HFs) share the same essential features of organization and function, and basic hair research in the mouse has long been both the foundation and at the forefront of our understanding of hair biology (Dry, 1926; Hsu *et al*., 2014; Montagna and Ellis, 1958; Plikus and Chuong, 2014; Schneider *et al*., 2009; Sundberg *et al*., 2005). In both species, HFs contain the same principal cell types and undergo repetitive cycling, alternating between phases of active growth (anagen), regression (catagen), and relative "quiescence" (telogen) (Geyfman *et al*., 2014; Paus and Cotsarelis, 1999; Schneider *et al*., 2009).

However, significant interspecies differences exist, limiting the translational potential of the murine HF model. Critically, anagen in the human scalp lasts for several years, whereas murine dorsal skin anagen is only 2–3 weeks long (Garza *et al*., 2012; Halloy *et al*., 2000; Müller-Röver *et al*., 2001), and epithelial HF stem cells differ in their markers and characteristics (Cotsarelis, 2006; Kloepper *et al*., 2008; Purba *et al*., 2014). Furthermore, while murine pelage HFs synchronize their cycles and grow in coordinated domains (Plikus *et al*., 2011; Plikus *et al*., 2008), human scalp HFs cycle asynchronously (mosaic, stochastically-driven hair cycle) (Dawber, 1997; Halloy *et al*., 2000) (see also Supplementary Text S1).

Although both human and murine HFs are exquisitely responsive to hormonal stimulation, their responses differ. For example, while estrogens and prolactin inhibit murine HF growth and cycling, both hormones prolong anagen duration in human female temporofrontal scalp HFs (Langan *et al*., 2010; Ohnemus *et al*., 2006). Thus, the response of murine HFs to stimulation with candidate hair growth-modulating agents does not necessarily predict how human HFs will respond, and may actually be misleading. Finally, the characteristic phenomenon of androgen-dependent HF miniaturization, seen in androgenetic alopecia (Dawber, 1997; Lattanand and Johnson, 1975), is not reproducible in currently available mouse strains (Crabtree *et al*., 2010; Nakamura *et al*., 2013; Sundberg *et al*., 1999).

The clinical importance of standardized human hair cycle staging

Considering that scalp skin harbors ca. 100,000 terminal HFs, even minor variations in their cycling have major clinical effects (Dawber, 1997). Thus, a small increase in the percentage of telogen scalp HFs by just a few percent can cause substantial effluvium, e.g. due to premature catagen induction by hormones, inflammatory mediators, neuropeptides, autoimmune reactions, cytotoxic drugs, psychoemotional stress, or malnutrition (reviewed in Atanaskova Mesinkovska and Bergfeld, 2013; Dawber, 1997; Paus, 2006; Paus and Cotsarelis, 1999; Paus and Foitzik, 2004; Paus *et al*., 2013; Shapiro, 2007). Moreover,

establishing an accurate anagen-to-catagen-to-telogen HF ratio is important for diagnosing the kind of alopecia at hand and for assessing its severity and progression. While the telogen-to-anagen ratio can be determined non-invasively via a phototrichogram, skin biopsies and histological staging are required to identify catagen HFs and to distinguish defined anagen sub-stages (Van Neste, 2002). Additionally, accurate histological hair cycle stage assessment is essential for quantitative preclinical and clinical hair research.

Therefore, an easy-to-follow, objective guide for the precise, standardized, and reproducible identification of human HF cycle stages is needed, ideally on the basis of routine histochemistry alone, without having to examine stage-specific molecular markers by immunohistochemistry, unless the latter provides crucial, otherwise unobtainable insights. While a comprehensive guide for murine hair cycle staging has long been available (Müller-Röver *et al*., 2001), the only major review on the human hair cycle dates back to 1959 (Kligman, 1959), yet it provides insufficient detail to guide accurate hair cycle staging. While this review has since been complemented by excellent atlases (e.g., Sperling *et al*., 2012; Whiting, 2004), and by a guide for evaluating the anagen-catagen transition of microdissected, organ-cultured human HFs *ex vivo* (Kloepper *et al*., 2010), a standardized, comprehensive, user-friendly, and electronically accessible human hair cycle guide *in vivo* is missing. The current study strives to provide this.

Standardized assessment of human HF cycling in the xenograft mouse model

HF xenotransplantation is currently the only preclinical assay that permits complete human HF cycling and supports long-lasting human anagen studies *in vivo* and is therefore a uniquely instructive and indispensable human hair research tool. However, despite several early reports (De Brouwer *et al*., 1997; Gilhar *et al*., 1988; Gilhar *et al*., 1998; Hashimoto *et al*., 2000, 2001; Jahoda *et al*., 1996; Krajcik *et al*., 2003; Lyle *et al*., 1999; Tang *et al*., 2002; Van Neste *et al*., 1989), and more recent uses for the experimental induction of alopecia areata (Gilhar *et al*., 2013), post-grafting human scalp hair cycle dynamics remain poorly characterized, hindering broader adaptation of this model. Furthermore, as xenografting is inevitably associated with surgery-, wound healing-, reinnervation-, and reperfusion-related phenomena that are absent during normal scalp HF cycling *in vivo* (see below), a detailed morphological comparison between xenografted and freshly biopsied human scalp HFs is needed. Because such a comparison has previously been unavailable, there is limited understanding of the extent to which human hair cycle events seen in host mice are representative of normal human hair cycle progression *in vivo*.

Therefore, this human hair cycle guide is complemented with a systematic analysis of HF cycling in xenografted human scalp skin, noting major similarities alongside minor differences and specific transplantation-related phenomena that one needs to be aware of. Finally, we report statistically validated, practical recommendations for designing human-on-mouse HF xenotransplantation experiments.

Results

Human hair cycle staging

HF cycle stages were evaluated based on the following histological characteristics (Supplementary Table S1): (i) size and shape of the dermal papilla (DP) and hair matrix, (ii) epithelial outer root sheath (ORS) morphology, (iii) connective sheath and vitreous membrane morphology, (iv) hair shaft characteristics, such as length and the presence of club, (v) the presence of the inner root sheath (IRS), (vi) pigment distribution, and (vii) the presence of apoptotic and/or proliferating cells, following the example of murine hair cycle staging (Müller-Röver *et al*., 2001). Additional markers can be assessed immunohistologically to demarcate selected cell populations or structures, such as epithelial stem cells or HF-associated keratins, but are dispensable for hair cycle staging (Supplementary Table S2).

Similar to routine hair transplantation in humans (Unger, 2005) or in chemotherapy-induced alopecia (Paus *et al*., 2013), xenografted anagen HFs (HFs-XG) predominantly enter catagen, thereby inducing a new hair cycle and allowing for quick recovery from surgery-associated damages. While these HFs-XG often shows signs of dystrophy ("dystrophic catagen"), less damaged HFs-XG enter into the "dystrophic anagen" damage-response pathway, with retarded progression into a new hair cycle (Paus *et al*., 2013). In the following sections, we first describe HF morphology in human scalp skin *in situ* (HF-IS) and subsequently explain the extent to which the hair cycle stages of HFs-XG recapitulate HFs-IS. Importantly, when staging HFs-IS, HF size and position relative to neighboring follicles and to epidermal/dermal or dermal/adipose tissue boundaries can be used as morphological landmarks. However, these landmarks cannot be recruited for hair cycle staging of HFs-XG.

Early catagen

This guide covers catagen first because after human HFs have completed their fetal morphogenesis (Montagna and Ellis, 1958), their life-long cycling activity begins with the first catagen entry *in utero*. For practical reasons, the eight distinct stages of catagen development in mice (Müller-Röver *et al*., 2001) are best subdivided into three, relatively easily recognizable stages (Kloepper *et al*., 2010): *early catagen*, equivalent to murine catagen phases I–IV; *mid catagen* (i.e. murine catagen V–VI); and *late catagen* (i.e. murine catagen VII–VIII) (Müller-Röver *et al*., 2001).

In HFs-IS, matrix and DP volume reduction, together with a complete cessation of HF pigmentation, are the earliest signs of catagen development that can be positively distinguished from anagen stage VI. Characteristically, the DP becomes more condensed and almond-shaped. Termination of melanogenesis (Bodo *et al*., 2007; Slominski *et al*., 2005; Tobin, 2011) results in the proximal end of the hair shaft becoming notably less pigmented than in anagen VI HFs (Figure 1a). Some melanin incontinence into the DP can also be seen, as the normal transfer of melanosomes into precortical hair matrix keratinocytes is interrupted (Tobin, 2011) (Figure 1b, feature #5). Importantly, morphology of the bulge region and the overall follicle length remain largely unchanged compared to anagen VI HFs-IS, and the lower HF portion rests below the dermal/adipose junction.

Positive staining for apoptotic cells (e.g. by caspase-3 or TUNEL immunofluorescence) in the regressing epithelium above the DP can be used as a definitive immunohistological marker of early catagen, since apoptotic cells are essentially undetectable in healthy anagen VI HFs *in vivo* (Botchkareva *et al*., 2006; Botchkareva *et al*., 2007; Sharova *et al*., 2014). Furthermore, downregulation of IRS and DP immunohistological markers can be used to differentiate early catagen HFs from anagen VI HFs (see Supplementary Table S2) (Commo and Bernard, 1997; Malgouries *et al*., 2008a; Malgouries *et al*., 2008b).

In HFs-XG, anagen VI progresses into catagen unusually rapidly so that on day two post-grafting, follicles that closely correspond to murine catagen stage IV can already be found (Müller-Röver *et al*., 2001) (Figure 1d–h). In catagen HFs-XG, the matrix is reduced down to just two-three cell layers, yet still envelops a small, almond-shaped DP (Figure 1f, 1g, feature #2). The newly forming club hair is located a short distance above the condensed DP (Figure 1f, 1g, feature #6). A significant portion (76.4%) of HFs-XG undergo “dystrophic catagen” (Paus *et al*., 2013), during which a normal, serrated club hair shaft fails to form, and the regressing hair matrix above the DP commonly contains ectopic melanin deposits (Supplementary Figure S1a–e, S3).

Mid-catagen

In HFs-IS and HFs-XG, the matrix and DP further decrease in volume – residual matrix is only 1–2 cell layers thick and only partially wraps around the condensed, almond-shaped DP (Figure 1i, features #1, 2). A brush-like club hair becomes prominent at this stage, and it resides above the dermal/adipose boundary (Figure 1i, 1p, feature #4). The newly formed epithelial strand (the remnant of the regressing hair matrix and proximal ORS) between the club hair and the DP is thin, generally lacks pigment, and can have a ruffled, zipper-like appearance (Figure 1i, 1o, 1p, feature #3). Compared to early catagen, mid-catagen HFs acquire visible thickening of the vitreous membrane of the connective sheath, which prominently stains for the glycoprotein, biglycan (Figure 1i, 1o, 1q, feature #5). Because the IRS regresses and disappears during catagen, its absence can be used to differentiate mid- to late catagen HFs from early anagen III HFs upon H&E (Commo and Bernard, 1997). Dystrophic mid-catagen HFs-XG either lack or have incompletely formed club hairs, and melanin clumps and vitreous membrane thickening are prominent (Supplementary Figure S1f–j, S3).

Late catagen

In both HFs-IS and HFs-XG, the matrix disappears, and the DP becomes condensed and ball-shaped (Figure 1r, 1y, feature #1). The club hair is now prominently visible (Figure 1r, 1z, feature #4), and the epithelial strand has shortened (about half the length of that of mid-catagen HFs) (Figure 1r, 1x, 1y, feature #3). The thickened connective sheath, which characteristically trails below the DP into the adipose tissue and can contain melanin clumps (in HFs-XG), becomes prominent at this stage (“dermal streamer”) (Figure 1r, feature #5). A few apoptotic cells can still be detected in the epithelial strand (Figure 1t, feature #6). Importantly, in late catagen, apoptotic cells can also be found in the shrinking sebaceous gland (Figure 1t, feature #7), like in mice (Lindner *et al*., 1997). Dystrophic late catagen HFs-XG display ectopic melanin deposition in the epithelium (Supplementary Figure S1k–o,

S3) and prominent pleats in the bulge region, which co-localize with CD200-positive epithelial progenitors (Figure 1x, 1z, feature #8).

Telogen

HFs with typical telogen morphology can be seen *in situ*, but are generally absent in xenografts. Their defining characteristics are: (i) positioning of the HF entirely above the dermal/adipose boundary (Figure 2a, feature #4), (ii) prominent unpigmented, serrated club hair (Figure 2a, feature #3), (iii) very compact, well-rounded DP separated from the club hair by a maximally shortened, unpigmented epithelial strand, the "secondary hair germ" (SHG) (Figure 2a, features #1, 2). Apoptotic cells are generally lacking (Figure 2c, feature #5).

However, consistent with previous reports (reviewed in Geyfman *et al*., 2014), a few dispersed (not clustered) proliferating cells can often be seen in the SHG and the distal epithelium of telogen HFs-IS (Figure 2c, feature #6). Thus, telogen HFs are not really "resting"; unfortunately, the functionally crucial distinction between "refractory" and "permissive" telogen HFs is not possible by histology, and the corresponding molecular signatures have only been characterized for murine telogen (see Geyfman *et al*., 2014). Importantly, human telogen HFs-IS can undergo exogen, the phase of active club hair shedding (Higgins *et al*., 2009; Stenn, 2005). Following exogen, HFs-IS enter kenogen, the telogen phase without club hair (Rebora and Guarrera, 2002), which can last for several months (Courtois *et al*., 1994).

Anagen I

Due to their relatively short duration, early stages of anagen can be quite difficult to identify *in situ*. One also needs to keep in mind that hair cycle staging describes a continuous and dynamic morphogenetic process in a discontinuous manner (only anagen VI and telogen are relatively stable stages; for detailed discussion see Bernard (2012)). Unlike *in situ*, anagen I is relatively common in xenografts, making this the model of choice for investigating the human telogen-anagen transformation. Anagen I HFs-XG display a hybrid morphology: (i) similar to late catagen, their bulge region's epithelium retains a pleated appearance (Figure 2g, feature #8); (ii) the SHG becomes triangular or crescent-shaped and wraps around the DP (Figure 2g–i, feature #7), which remains condensed and ball-like, may contain melanin clumps (i.e., pigment residue from the preceding anagen VI stage) (Figure 2i, feature #9), and still shows a trailing connective sheath (Figure 2h, feature #1).

Anagen II

In HFs-IS and HFs-XG, the SHG undergoes proliferation-driven thickening and elongation (Figure 2k–t). Its proximal end develops into a new hair matrix, which at this stage is still unpigmented, crescent-shaped, and only partially encloses a small, yet slightly larger, less densely packed, ball-shaped DP (Figure 2k, 2q–s, features #1, 2). Proliferation markers reveal localized clusters of proliferating cells in the thickening hair germ (Figure 2m, feature #4), while apoptotic cells are lacking. The entire length of stage II anagen HFs-IS resides above the dermal/adipose boundary. In HFs-XG, the bulge region's epithelium retains its

pleated appearance (Figure 2r, 2t, feature #6), and the DP still contains melanin deposits (Figure 2s, feature #5).

Anagen III

In both HFs-IS and HFs-XG, the hair matrix has now formed and is 4–5 cell layers thick. It encloses at least 60% of the DP, which becomes enlarged and oval-shaped (Figure 3a, 3g–k, feature #2). Prominently, at this stage, HFs develop a hair shaft and IRS, both of which are easily identifiable in routine H&E stains (Figure 3a, 3b, 3g, 3i, 3k, feature #3). Immunostaining for proliferation markers reveals actively dividing cells both in the hair matrix and in the ORS (Figure 3c, 3j, feature #5). *In situ*, the hair bulb now reaches and extends into the adipose layer. In both HFs-IS and HFs-XG, three anagen III sub-stages can be differentiated based on hair shaft appearance. Anagen IIIa shafts lack a visible cortex (Figure 3g). Anagen IIIb and IIIc shafts have a visible cortex, while anagen IIIc hair shafts are long, reaching approximately twice the length of the hair matrix (Figure 3k). Importantly, throughout anagen III, hair shafts still lack visible pigmentation, even though HF melanogenesis in the HF pigmentary unit commences in anagen IIIc (Slominski *et al.*, 2005). Lastly, the bulge epithelium of HFs-XG retains a pleated appearance (Figure 3i, 3k, feature #6), and the DP still contains occasional melanin clumps.

Anagen IV

At this stage, the hair shaft is fully mature, with a distinct medulla (in terminal HFs), cortex, and cuticle easily identifiable on H&E, and the hair tip reaches the level of the sebaceous gland duct (Figure 4a–h, feature #5). Importantly, melanin production and transfer are now fully reactivated, and hair shafts become visibly pigmented. *In situ*, the hair bulb now reaches down to the upper dermal adipose layer (Figure 4a, feature #2), and a distinct connective sheath trail is visible proximal to the bulb, which guides further HF downgrowth (Figure 4a, feature #7).

Anagen V

In situ, the hair bulb extends further into the adipose layer, and the connective sheath trail disappears at this stage (Figure 4i, feature #2). In both HFs-IS and HFs-XG, the tip of the hair shaft enters the hair canal (Figure 4i, 4j, 4k, feature #5). The DP is now onion-shaped, and in the hair matrix, pigmentation reaches down to Auber's line (Figure 4l, 4m, features #1, 2, 6). Additionally, in HFs-XG, bulge epithelium contours begin to smoothen (Figure 4l, feature #8).

Anagen VI

The vast majority of HFs *in situ* are in anagen stage VI. The hair bulb is located deep in the dermal adipose layer, while the hair shaft emerges above the skin level (Figure 4p–w). In pigmented HFs, the hair matrix contains the maximum amount of melanin, which now reaches below Auber's line. In HFs-XG, bulge epithelium smoothens, but residual undulations, which can be homologous to the “follicular trochanter” in HFs-IS (Tiede *et al.*, 2007), can persist (Figure 4u, feature #8). Compared to anagen V, the DP is maximally enriched in extracellular matrix.

Practical recommendations for the xenograft model

Long-term survival of individually grafted human scalp HFs is much more consistent in SCID mice, averaging between 55–67% (Supplementary Figure S6d). In nude mice, it was extremely variable, ranging from 0% to 82%, likely reflecting mouse-to-mouse variability in graft rejection (Supplementary Figure S4). Also, among actively cycling HFs-XG, average hair growth rates are faster and more consistent in SCID than in nude mice (Supplementary Figure S6c). This confirms that SCID mice are the host of choice for xenografted human scalp HFs (Gilhar *et al.*, 2013; Gilhar *et al.*, 1998).

Xenograft transplantation provides a strong stimulus for catagen induction, thereby partially synchronizing hair cycling behavior (Figure 5). However, significant hair cycle stage heterogeneity is retained during all post-grafting time points (Figure 5b, 5c, 5d), demonstrating that the mosaicism of human HF cycling is partially maintained even after transplantation. We recommend using statistically adjusted peak time points generated here (see Figure 5e; Supplementary Figure S5) to evaluate the post-grafting human hair cycle. Moreover, because the majority of HFs-XG enter anagen stage VI on day 92, studies on anagen should be performed after this time point.

Discussion

Here, we provide a guide for staging terminal human scalp HFs *in situ* and in xenografts (Supplementary Figure S2) on the basis of a minimal set of characteristics, identifiable on routine histology. Depending on the specific hair research question(s) asked, additional standard read-out parameters can be employed that make the analysis of human HFs even more instructive, and Supplementary Table S2 lists selected examples for further guidance (Purba *et al.*, 2014; Purba *et al.*, 2015).

The mouse xenotransplant model remains indispensable for studying and experimentally manipulating human HF cycling *in vivo*. Besides follicular unit transplantation, as in the current study, one can also transplant carefully trimmed full-thickness scalp skin (Gilhar *et al.*, 2013; Gilhar *et al.*, 1998; Sintov *et al.*, 2000; Van Neste *et al.*, 1989). This greatly reduces the level of surgery-related damage suffered by HFs located away from the transplant edge and has the added advantage of permitting one to study the cycling behavior of an entire HF field as well as terminal HFs alongside vellus HFs, complete with associated sebaceous and sweat glands. However, perfusion, oxygenation, and re-innervation can be precarious in the center of such full-thickness transplants.

When interpreting data obtained with the xenotransplant model, one must keep in mind a number of confounding factors that may influence the results profoundly. Namely, xenotransplanted human HFs are re-perfused and re-innervated by cells and structures derived from an alien host and are shock-exposed to and must rapidly adjust to the foreign endocrine, innate immune, and metabolic system of SCID mice. In addition, the murine host launches a stress response to the trauma of surgery (note that perceived stress in mice triggers substantial perifollicular neurogenic inflammation, which is NGF-, substance P- and mast cell-dependent, centers around the bulge, and prematurely induces catagen in murine anagen HFs (Arck *et al.*, 2005)). Coupled with the fact that human scalp HFs also respond to

key stress-mediators (reviewed in Paus *et al.*, 2014), all of these confounding factors are expected to impact greatly on human HF cycling, growth, immune status, pigmentation, and metabolism *in vivo* after xenotransplantation. Therefore, caution is advised in extrapolating from observations made with human HF xenotransplants in mice to the response of healthy human scalp skin.

At any given time, the vast majority of asynchronously cycling HFs in healthy human scalp are considered to be in anagen (80–90%), between 10–20% in telogen, and only 1–5 % in catagen (Dawber, 1997; Shapiro, 2007; Sperling *et al.*, 2012; Whiting, 2004). However, our current histological analysis of HFs-IS suggests that the number of catagen HFs can exceed that of telogen HFs (catagen: 5–10%, telogen: 1–2%). This discrepancy likely reflects differences in assessment methodologies, since phototrichograms cannot distinguish between telogen and catagen and are thus less accurate compared to histology-based hair cycle staging (Hoffmann, 2001; Van Neste and Trueb, 2006). Additional histomorphometric hair cycle staging will be required to refine the true anagen:catagen:telogen scalp HF ratio. Due to the relatively short duration of anagen I to V, these anagen stages are rarely found *in situ*, with the notable exception of the weeks following extensive telogen effluvium, when a surge in premature anagen termination is followed by semi-synchronous anagen reactivation (Hadshiew *et al.*, 2004; Harrison and Sinclair, 2002; Katz *et al.*, 2006). Thus, an unusually high percentage of anagen stage I to V HFs points towards a preceding telogen effluvium.

Unlike *in situ*, anagen I-V HFs can be readily identified in xenografts due to a telogen effluvium-like resetting effect from the traumatic transplantation procedure (Gilhar *et al.*, 1988; Hashimoto *et al.*, 2000, 2001; Jahoda *et al.*, 1996; Van Neste *et al.*, 1989), complicated by various degrees of HF dystrophy, just as after chemotherapy (Paus *et al.*, 1994; Paus *et al.*, 2013). This resetting, however, is incomplete. While individual xenotransplanted anagen HFs rapidly enter catagen by day 3, their progression through catagen is variable, and late catagen HFs can still be found on day 50. This likely reflects variable response to trauma, when some HFs enter into normal, but premature catagen or the “dystrophic catagen”, while others undergo a “dystrophic anagen”, which protracts catagen development (Hendrix *et al.*, 2005; Paus *et al.*, 2013). This variable timing of the catagen program leads to incomplete hair cycle synchronization, heralding the reestablishment of cycling mosaicism. Additionally, grafted HFs do not appear to enter long-lasting telogen, suggesting that the normal HF stem cell quiescence mechanisms (Geyfman *et al.*, 2014; Mardaryev *et al.*, 2011) may be altered, perhaps as a result of the confounding, host-derived factors summarized above.

SCID mouse xenotransplantation model optimization for studying human anagen

Despite limitations of the xenograft model, HFs-XG closely resemble cycling HFs-IS and are able to enter long-lasting anagen. Therefore, the SCID mouse xenograft model (see also Gilhar *et al.*, 2013; Gilhar *et al.*, 1998) provides an extremely valuable experimental system for investigating multiple, otherwise difficult-to-study aspects of human HF biology, and instructively complements *in vitro* human HF and scalp skin organ culture (Al-Nuaimi *et al.*, 2014; Hardman *et al.*, 2015; Kloepper *et al.*, 2010; Lu *et al.*, 2007; Oh *et al.*, 2013; Philpott *et al.*, 1990; Poeggeler *et al.*, 2010). We recommend using at least three post-grafting time

points to study catagen-to-anagen progression, and waiting until after post-grafting 92 days for studying anagen VI HFs. This is substantially later than the post-grafting days 60–70 reported previously (Hashimoto *et al.*, 2000, 2001). Future studies wishing to investigate human HF responses to hormonal stimulation, e.g. in the context of androgenetic alopecia, also need to consider the intricate hormone-sensitivity of human HFs (Paus *et al.*, 2014) and their keratin expression patterns (Ramot and Paus, 2014); therefore, imitating donor-like hormone levels in host mice (e.g. testosterone) is important (De Brouwer *et al.*, 1997; Krajcik *et al.*, 2003; Sintov *et al.*, 2000; Van Neste *et al.*, 1991).

In summary, while *Mus musculus* remains unrivaled in the insights it has helped to generate into basic HF biology, murine HF physiology is quite different from that of human HF. The xenotransplant model characterized above provides an indispensable tool for human preclinical hair research *in vivo*, if employed together with the comprehensive guide for human hair cycle staging developed here.

Materials and Methods

Human scalp hair follicles and xenografting

Institutional approval and written informed patient consent were received for all studies using human tissue samples, and institutional approval was received for all animal studies. Human scalp skin *in situ* studies were performed on normal occipital and temporal scalp skin samples following previously published protocols (Harries *et al.*, 2013; Harries and Paus, 2010; Kloepper *et al.*, 2010). For xenografting, non-balding occipital scalp skin specimens were used. The method for human HF xenografting was adapted after Hashimoto *et al.* (2000). Briefly, 15 to 40 (on average 25) microdissected anagen VI follicular units were transplanted onto 6–8 weeks old female nude or SCID mice (Jackson Laboratory, Bar Harbor, Maine, USA). A total of 1,164 HFs were transplanted and then biopsied and analyzed at 45 consecutive time points (see Supplementary Table S3 and Supplementary Materials and Methods).

Histological tissue analysis

Paraffin embedded HF samples were sectioned at 3um thickness, and O.C.T compound embedded follicles were sectioned at 8um under −20°C. Sections were processed either for routine histology (H&E staining) or for immunofluorescence staining (see Supplementary Materials and Methods).

Computational analysis and statistical tests

Hair cycle stage's mean date was determined by averaging the time points when biopsied HFs were at the corresponding stage. To estimate the time point with the greatest probability of selecting a HF in the desired stage, the naïve Bayes classifier (Mitchell, 1997) was used. Additional computer simulations were employed to derive probability values for each hair cycle stage, and two-sample Kolmogorov-Smirnov (K-S) test (Conover, 1999) was utilized to compare the speed of HF-XG hair cycle progression between nude and SCID host mice (see Supplementary Materials and Methods for details).

Supplementary Material

Refer to Web version on PubMed Central for supplementary material.

Acknowledgements

JWO is supported by the Regenerative Medicine R&D fund provided by Daegu city (Korea), and ETRI R&D Program (15ZC3100). MVP is supported by the NIH National Institute of Arthritis and Musculoskeletal and Skin Diseases (NIAMS) grant R01-AR067273, Edward Mallinckrodt Jr. Foundation grant and University of California Cancer Research Coordinating Committee (CRCC) grant. This research was also supported by the Basic Science Research Program through the National Research Foundation of Korea (NRF) funded by the Ministry of Education, Science and Technology (NRF-2012R1A1B3001047 to YKS and NRF-2014R1A5A2009242 to MK), and by a grant from Deutsche Forschungsgemeinschaft (Pa 345/13-1) to RP. The authors are most grateful and indebted to many colleagues, who generously lent a helping hand and/or provided expert advice during some stage of this long-lasting expedition into human hair cycle staging, in particular to Sang In Choi, Chang Hoon Seo, Mi Hee Kwack, Seung Hyun Shin, Sanguk Im, Jin Oh Kim Dorothee Langan, Koji Sugawara, David Whiting, George Cotsarelis, Nadine Dörwald, Jonathan Le and Manda Nguyen.

References

Al-Nuaimi Y, Hardman JA, Biro T, et al. A meeting of two chronobiological systems: circadian proteins Period1 and BMAL1 modulate the human hair cycle clock. The Journal of investigative dermatology. 2014; 134:610–9. [PubMed: 24005054]

Arck PC, Handjiski B, Kuhlmei A, et al. Mast cell deficient and neurokinin-1 receptor knockout mice are protected from stress-induced hair growth inhibition. J Mol Med (Berl). 2005; 83:386–96. [PubMed: 15759104]

Atanaskova Mesinkovska N, Bergfeld WF. Hair: what is new in diagnosis and management? Female pattern hair loss update: diagnosis and treatment. Dermatol Clin. 2013; 31:119–27. [PubMed: 23159181]

Bernard BA. The human hair follicle, a bistable organ? Experimental dermatology. 2012; 21:401–3. [PubMed: 22458655]

Bodo E, Tobin DJ, Kamenisch Y, et al. Dissecting the impact of chemotherapy on the human hair follicle: a pragmatic in vitro assay for studying the pathogenesis and potential management of hair follicle dystrophy. Am J Pathol. 2007; 171:1153–67. [PubMed: 17823286]

Botchkareva NV, Ahluwalia G, Shander D. Apoptosis in the hair follicle. The Journal of investigative dermatology. 2006; 126:258–64. [PubMed: 16418734]

Botchkareva NV, Kahn M, Ahluwalia G, et al. Survivin in the human hair follicle. The Journal of investigative dermatology. 2007; 127:479–82. [PubMed: 16946715]

Commo S, Bernard BA. Immunohistochemical analysis of tissue remodelling during the anagen-catagen transition of the human hair follicle. The British journal of dermatology. 1997; 137:31–8. [PubMed: 9274622]

Conover, WJ. Practical nonparametric statistics. 3rd edn. Wiley; New York: 1999. p. viiip. 584

Cotsarelis G. Gene expression profiling gets to the root of human hair follicle stem cells. The Journal of clinical investigation. 2006; 116:19–22. [PubMed: 16395398]

Courtois M, Loussouarn G, Hourseau C, et al. Hair cycle and alopecia. Skin Pharmacol. 1994; 7:84–9. [PubMed: 8003330]

Crabtree JS, Kilbourne EJ, Peano BJ, et al. A mouse model of androgenetic alopecia. Endocrinology. 2010; 151:2373–80. [PubMed: 20233794]

Dawber, RPR. Diseases of the Hair and Scalp. Wiley; 1997.

De Brouwer B, Tetelin C, Leroy T, et al. A controlled study of the effects of RU58841, a non-steroidal antiandrogen, on human hair production by balding scalp grafts maintained on testosterone-conditioned nude mice. The British journal of dermatology. 1997; 137:699–702. [PubMed: 9415227]

Dry FW. The coat of the mouse (Mus musculus). Journ of Gen. 1926; 16:287–340.

Garza LA, Liu Y, Yang Z, et al. Prostaglandin D2 inhibits hair growth and is elevated in bald scalp of men with androgenetic alopecia. Science translational medicine. 2012; 4 126ra34.

Geyfman, M.; Plikus, MV.; Treffeisen, E., et al. Biol Rev Camb Philos Soc. 2014. Resting no more: re-defining telogen, the maintenance stage of the hair growth cycle.

Gilhar A, Keren A, Shemer A, et al. Autoimmune disease induction in a healthy human organ: a humanized mouse model of alopecia areata. The Journal of investigative dermatology. 2013; 133:844–7. [PubMed: 23096715]

Gilhar A, Pillar T, Etzioni A. The effect of topical cyclosporin on the immediate shedding of human scalp hair grafted onto nude mice. The British journal of dermatology. 1988; 119:767–70. [PubMed: 3203070]

Gilhar A, Ullmann Y, Berkutzki T, et al. Autoimmune hair loss (alopecia areata) transferred by T lymphocytes to human scalp explants on SCID mice. The Journal of clinical investigation. 1998; 101:62–7. [PubMed: 9421466]

Hadshiew IM, Foitzik K, Arck PC, et al. Burden of hair loss: stress and the underestimated psychosocial impact of telogen effluvium and androgenetic alopecia. The Journal of investigative dermatology. 2004; 123:455–7. [PubMed: 15304082]

Halloy J, Bernard BA, Loussouarn G, et al. Modeling the dynamics of human hair cycles by a follicular automaton. Proc Natl Acad Sci U S A. 2000; 97:8328–33. [PubMed: 10899998]

Hardman JA, Tobin DJ, Haslam IS, et al. The peripheral clock regulates human pigmentation. The Journal of investigative dermatology. 2015; 135:1053–64. [PubMed: 25310406]

Harries MJ, Meyer K, Chaudhry I, et al. Lichen planopilaris is characterized by immune privilege collapse of the hair follicle's epithelial stem cell niche. J Pathol. 2013; 231:236–47. [PubMed: 23788005]

Harries MJ, Paus R. The pathogenesis of primary cicatricial alopecias. Am J Pathol. 2010; 177:2152–62. [PubMed: 20889564]

Harrison S, Sinclair R. Telogen effluvium. Clin Exp Dermatol. 2002; 27:389–5. [PubMed: 12190639]

Hashimoto T, Kazama T, Ito M, et al. Histologic and cell kinetic studies of hair loss and subsequent recovery process of human scalp hair follicles grafted onto severe combined immunodeficient mice. The Journal of investigative dermatology. 2000; 115:200–6. [PubMed: 10951236]

Hashimoto T, Kazama T, Ito M, et al. Histologic study of the regeneration process of human hair follicles grafted onto SCID mice after bulb amputation. The journal of investigative dermatology Symposium proceedings / the Society for Investigative Dermatology, Inc [and] European Society for Dermatological Research. 2001; 6:38–42.

Hendrix S, Handjiski B, Peters EM, et al. A guide to assessing damage response pathways of the hair follicle: lessons from cyclophosphamide-induced alopecia in mice. The Journal of investigative dermatology. 2005; 125:42–51. [PubMed: 15982301]

Higgins CA, Westgate GE, Jahoda CA. From telogen to exogen: mechanisms underlying formation and subsequent loss of the hair club fiber. The Journal of investigative dermatology. 2009; 129:2100–8. [PubMed: 19340011]

Hoffmann R. TrichoScan: combining epiluminescence microscopy with digital image analysis for the measurement of hair growth in vivo. Eur J Dermatol. 2001; 11:362–8. [PubMed: 11399546]

Hsu YC, Li L, Fuchs E. Emerging interactions between skin stem cells and their niches. Nat Med. 2014; 20:847–56. [PubMed: 25100530]

Jahoda CA, Oliver RF, Reynolds AJ, et al. Human hair follicle regeneration following amputation and grafting into the nude mouse. The Journal of investigative dermatology. 1996; 107:804–7. [PubMed: 8941664]

Katz KA, Cotsarelis G, Gupta R, et al. Telogen effluvium associated with the dopamine agonist pramipexole in a 55-year-old woman with Parkinson's disease. Journal of the American Academy of Dermatology. 2006; 55:S103–4. [PubMed: 17052518]

Kligman AM. The human hair cycle. The Journal of investigative dermatology. 1959; 33:307–16. [PubMed: 14409844]

Kloepper JE, Sugawara K, Al-Nuaimi Y, et al. Methods in hair research: how to objectively distinguish between anagen and catagen in human hair follicle organ culture. Experimental dermatology. 2010; 19:305–12. [PubMed: 19725870]

Kloepper JE, Tiede S, Brinckmann J, et al. Immunophenotyping of the human bulge region: the quest to define useful in situ markers for human epithelial hair follicle stem cells and their niche. Experimental dermatology. 2008; 17:592–609. [PubMed: 18558994]

Krajcik RA, Vogelman JH, Malloy VL, et al. Transplants from balding and hairy androgenetic alopecia scalp regrow hair comparably well on immunodeficient mice. Journal of the American Academy of Dermatology. 2003; 48:752–9. [PubMed: 12734505]

Langan EA, Foitzik-Lau K, Goffin V, et al. Prolactin: an emerging force along the cutaneous-endocrine axis. Trends Endocrinol Metab. 2010; 21:569–77. [PubMed: 20598901]

Lattanand A, Johnson WC. Male pattern alopecia a histopathologic and histochemical study. Journal of cutaneous pathology. 1975; 2:58–70. [PubMed: 777055]

Lindner G, Botchkarev VA, Botchkareva NV, et al. Analysis of apoptosis during hair follicle regression (catagen). Am J Pathol. 1997; 151:1601–17. [PubMed: 9403711]

Lu Z, Hasse S, Bodo E, et al. Towards the development of a simplified long-term organ culture method for human scalp skin and its appendages under serum-free conditions. Experimental dermatology. 2007; 16:37–44. [PubMed: 17181635]

Lyle S, Christofidou-Solomidou M, Liu Y, et al. Human hair follicle bulge cells are biochemically distinct and possess an epithelial stem cell phenotype. The journal of investigative dermatology Symposium proceedings / the Society for Investigative Dermatology, Inc [and] European Society for Dermatological Research. 1999; 4:296–301.

Malgouries S, Donovan M, Thibaut S, et al. Heparanase 1: a key participant of inner root sheath differentiation program and hair follicle homeostasis. Experimental dermatology. 2008a; 17:1017–23. [PubMed: 18557927]

Malgouries S, Thibaut S, Bernard BA. Proteoglycan expression patterns in human hair follicle. The British journal of dermatology. 2008b; 158:234–42. [PubMed: 18067481]

Mardaryev AN, Meier N, Poterlowicz K, et al. Lhx2 differentially regulates Sox9, Tcf4 and Lgr5 in hair follicle stem cells to promote epidermal regeneration after injury. Development. 2011; 138:4843–52. [PubMed: 22028024]

Mitchell, TM. Machine Learning. McGraw-Hill; New York: 1997. p. xviip. 414

Montagna, W.; Ellis, RA. The biology of hair growth. Academic Press; 1958.

Müller-Röver S, Handjiski B, van der Veen C, et al. A comprehensive guide for the accurate classification of murine hair follicles in distinct hair cycle stages. The Journal of investigative dermatology. 2001; 117:3–15. [PubMed: 11442744]

Nakamura M, Schneider MR, Schmidt-Ullrich R, et al. Mutant laboratory mice with abnormalities in hair follicle morphogenesis, cycling, and/or structure: an update. J Dermatol Sci. 2013; 69:6–29. [PubMed: 23165165]

Oh JW, Hsi TC, Guerrero-Juarez CF, et al. Organotypic skin culture. The Journal of investigative dermatology. 2013; 133:e14. [PubMed: 24129782]

Ohnemus U, Uenalan M, Inzunza J, et al. The hair follicle as an estrogen target and source. Endocr Rev. 2006; 27:677–706. [PubMed: 16877675]

Paus R. Therapeutic strategies for treating hair loss. Drug Discovery Today: Therapeutic Strategies. 2006; 3:101–10.

Paus R, Cotsarelis G. The biology of hair follicles. The New England journal of medicine. 1999; 341:491–7. [PubMed: 10441606]

Paus R, Foitzik K. In search of the “hair cycle clock”: a guided tour. Differentiation. 2004; 72:489–511. [PubMed: 15617561]

Paus R, Handjiski B, Eichmuller S, et al. Chemotherapy-induced alopecia in mice. Induction by cyclophosphamide, inhibition by cyclosporine A, and modulation by dexamethasone. Am J Pathol. 1994; 144:719–34. [PubMed: 8160773]

Paus R, Haslam IS, Sharov AA, et al. Pathobiology of chemotherapy-induced hair loss. Lancet Oncol. 2013; 14:e50–9. [PubMed: 23369683]

Paus R, Langan EA, Vidali S, et al. Neuroendocrinology of the hair follicle: principles and clinical perspectives. Trends Mol Med. 2014; 20:559–70. [PubMed: 25066729]

Philpott MP, Green MR, Kealey T. Human hair growth in vitro. Journal of cell science. 1990; 97(Pt 3): 463–71. [PubMed: 1705941]

Plikus MV, Baker RE, Chen CC, et al. Self-organizing and stochastic behaviors during the regeneration of hair stem cells. Science. 2011; 332:586–9. [PubMed: 21527712]

Plikus MV, Chuong CM. Macroenvironmental regulation of hair cycling and collective regenerative behavior. Cold Spring Harb Perspect Med. 2014; 4 a015198.

Plikus MV, Mayer JA, de la Cruz D, et al. Cyclic dermal BMP signalling regulates stem cell activation during hair regeneration. Nature. 2008; 451:340–4. [PubMed: 18202659]

Poeggeler B, Bodo E, Nadrowitz R, et al. A simple assay for the study of human hair follicle damage induced by ionizing irradiation. Experimental dermatology. 2010; 19:e306–9. [PubMed: 19925637]

Purba TS, Haslam IS, Poblet E, et al. Human epithelial hair follicle stem cells and their progeny: current state of knowledge, the widening gap in translational research and future challenges. BioEssays : news and reviews in molecular, cellular and developmental biology. 2014; 36:513–25.

Purba TS, Haslam IS, Shahmalak A, et al. Mapping the expression of epithelial hair follicle stem cell-related transcription factors LHX2 and SOX9 in the human hair follicle. Experimental dermatology. 2015; 24:462–7. [PubMed: 25808706]

Ramot Y, Paus R. Harnessing neuroendocrine controls of keratin expression: a new therapeutic strategy for skin diseases? BioEssays : news and reviews in molecular, cellular and developmental biology. 2014; 36:672–86.

Rebora A, Guarrera M. Kenogen. A new phase of the hair cycle? Dermatology. 2002; 205:108–10. [PubMed: 12218222]

Schneider MR, Schmidt-Ullrich R, Paus R. The hair follicle as a dynamic miniorgan. Curr Biol. 2009; 19:R132–42. [PubMed: 19211055]

Shapiro J. Clinical practice. Hair loss in women. The New England journal of medicine. 2007; 357:1620–30. [PubMed: 17942874]

Sharova TY, Poterlowicz K, Botchkareva NV, et al. Complex changes in the apoptotic and cell differentiation programs during initiation of the hair follicle response to chemotherapy. The Journal of investigative dermatology. 2014; 134:2873–82. [PubMed: 24999588]

Sintov A, Serafimovich S, Gilhar A. New topical antiandrogenic formulations can stimulate hair growth in human bald scalp grafted onto mice. Int J Pharm. 2000; 194:125–34. [PubMed: 10601691]

Slominski A, Wortsman J, Plonka PM, et al. Hair follicle pigmentation. The Journal of investigative dermatology. 2005; 124:13–21. [PubMed: 15654948]

Sperling, LC.; Cowper, SE.; Knopp, EA. An Atlas of Hair Pathology with Clinical Correlations, Second Edition. Taylor & Francis; 2012.

Stenn K. Exogen is an active, separately controlled phase of the hair growth cycle. Journal of the American Academy of Dermatology. 2005; 52:374–5. [PubMed: 15692497]

Sundberg JP, Beamer WG, Uno H, et al. Androgenetic alopecia: in vivo models. Exp Mol Pathol. 1999; 67:118–30. [PubMed: 10527763]

Sundberg JP, Peters EM, Paus R. Analysis of hair follicles in mutant laboratory mice. The journal of investigative dermatology Symposium proceedings / the Society for Investigative Dermatology, Inc [and] European Society for Dermatological Research. 2005; 10:264–70.

Tang L, Madani S, Lui H, et al. Regeneration of a new hair follicle from the upper half of a human hair follicle in a nude mouse. The Journal of investigative dermatology. 2002; 119:983–4. [PubMed: 12406351]

Tiede S, Kloepper JE, Whiting DA, et al. The `follicular trochanter': an epithelial compartment of the human hair follicle bulge region in need of further characterization. The British journal of dermatology. 2007; 157:1013–6. [PubMed: 17714535]

Tobin DJ. The cell biology of human hair follicle pigmentation. Pigment Cell Melanoma Res. 2011; 24:75–88. [PubMed: 21070612]

Unger WP. Hair transplantation: current concepts and techniques. The journal of investigative dermatology Symposium proceedings / the Society for Investigative Dermatology, Inc [and] European Society for Dermatological Research. 2005; 10:225–9.

Van Neste D, De Brouwer B, Dumortier M. Reduced linear hair growth rates of vellus and of terminal hairs produced by human balding scalp grafted onto nude mice. Annals of the New York Academy of Sciences. 1991; 642:480–2. [PubMed: 1809113]

Van Neste D, Trueb RM. Critical study of hair growth analysis with computer-assisted methods. J Eur Acad Dermatol Venereol. 2006; 20:578–83. [PubMed: 16684287]

Van Neste, D.; Warnier, G.; Thulliez, M., et al. Human hair follicle grafts onto nude mice: morphological study. In: Van Neste, D.; Lachapelle, JM.; Antoine, JL., editors. Trends in Human Hair Growth and Alopecia Research. Springer Netherlands; 1989. p. 117-31.

Van Neste MD. Assessment of hair loss: clinical relevance of hair growth evaluation methods. Clin Exp Dermatol. 2002; 27:358–65. [PubMed: 12190635]

Whiting, DA. The Structure of the Human Hair Follicle: Light Microscopy of Vertical and Horizontal Sections of Scalp Biopsies. Canfield Publishing; 2004.

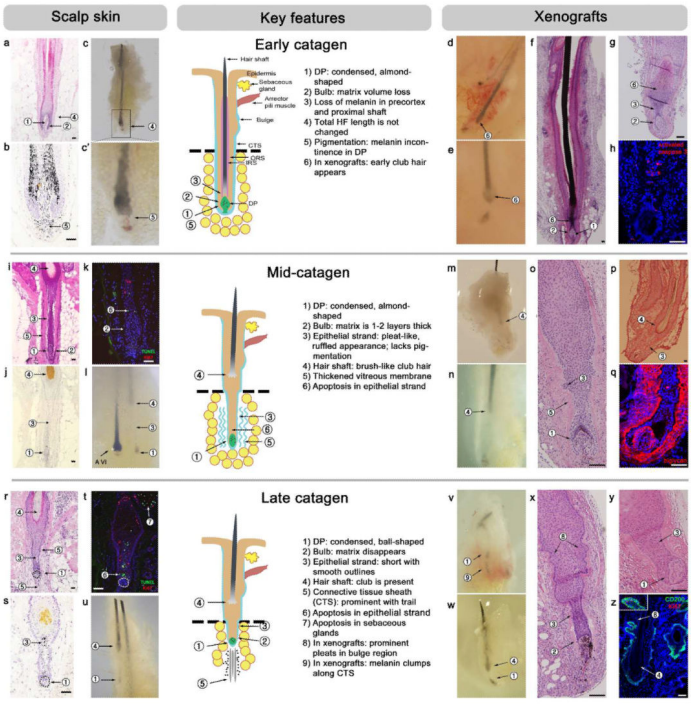

408x415mm (300 x 300 DPI)

Figure 1. Catagen

For practical reasons, catagen was subdivided into three, easily recognizable stages: early, mid-, and late catagen. For each stage, a schematic drawing is provided, with key and auxiliary features numbered and marked. For HFs-IS, 5–10% of all HFs are in catagen. In xenografts, approximately three quarters of HFs-XG undergo “dystrophic catagen”, during which a club hair fails to form (see Supplementary Figure S1).

(a–h) Early catagen in HFs-IS (a-c') and HFs-XG (d-h). Key features at this stage are matrix volume loss, loss of pigment at the proximal end of the hair shaft, melanin incontinence into the DP, and the appearance of apoptotic cells. On *in situ*, HF length remains unchanged compared to anagen VI HFs. In xenografts, the peak day for early catagen is post-grafting day 3.

(i–q) Mid-catagen in HFs-IS (i-l) and HFs-XG (m-q). Key features at this stage are a shrinking matrix, which is only 1–2 cell layers thick, thin epithelial strand with pleated outlines and apoptotic cells, presence of the brush-like club hair, and a thick vitreous membrane. On *in situ*, the proximal portion of the HF is still within the adipose layer. In xenografts, the peak day for mid-catagen is post-grafting day 18.

(r–z) Late catagen in HFs-IS (r-u) and HFs-XG (v-z). Key features at this stage are a smaller, ball-shaped DP, absence of the hair matrix, shortened (compared to mid-catagen) epithelial strand, prominent connective tissue sheath with the trail below the DP, melanin clumps in the trail, and ongoing apoptosis in the epithelial strand. Additionally, on *in situ*, apoptosis occurs in the sebaceous gland. In xenografts, the bulge region develops prominent pleats. This stage peaks on post-grafting day 29.

Hosts: SCID mice (panels - e, g, j, m, q, x, y), nude mice (panels - d, f, h, n, o, p, v, w, z). Scale bars: 100 um.

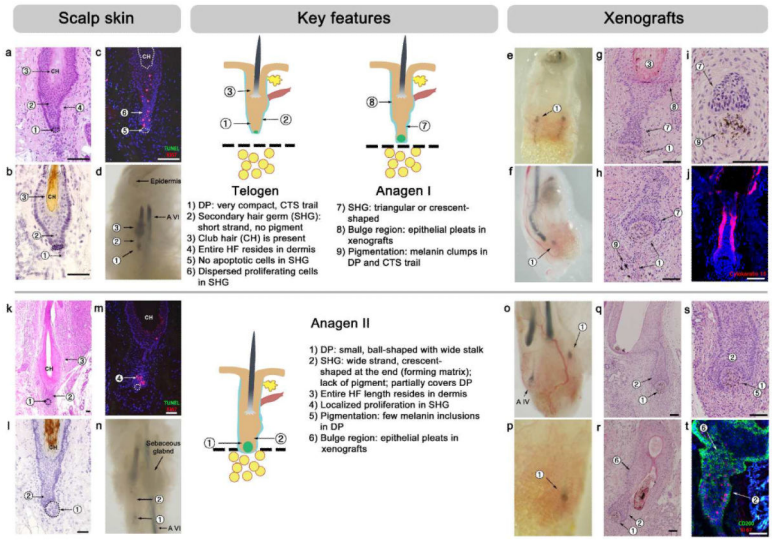

414x289mm (300 x 300 DPI)

Figure 2. Telogen and anagen I, II

For each stage, a schematic drawing is provided, and key and auxiliary features are numbered and marked.

(a–d) Telogen. HFs with typical telogen morphology represent 1–2% of all HFs on *in situ* findings and are generally lacking in xenografts. Key features at this stage are a very small DP and a short secondary hair germ that lacks apoptotic cells. The entire length of the telogen HF rests in the dermis.

(e–j) Anagen I. HFs with anagen I morphology are generally not found *in situ* but are common in xenografts, peaking on post-grafting day 33. Key features at this stage are a small DP, a secondary hair germ shaped as triangle or small crescent, and an initiation of proliferation at the base of the germ.

(k–t) Anagen II in HFs-IS (k-n) and HFs-XG (o-t). Key features at this stage are a small DP with a wide stalk (compared to telogen and anagen I), an enlarged secondary hair germ with prominent crescent shape, and a localized proliferation hotspot at the base of the germ. On *in situ*, the entire length of the HF rests in the dermis. In xenografts, the peak day for anagen II is post-grafting day 40.

Hosts: SCID mice (panels - f, g, h, j, o, q, r, s), nude mice (panels - e, i, p, t).

Scale bars: 100 um.

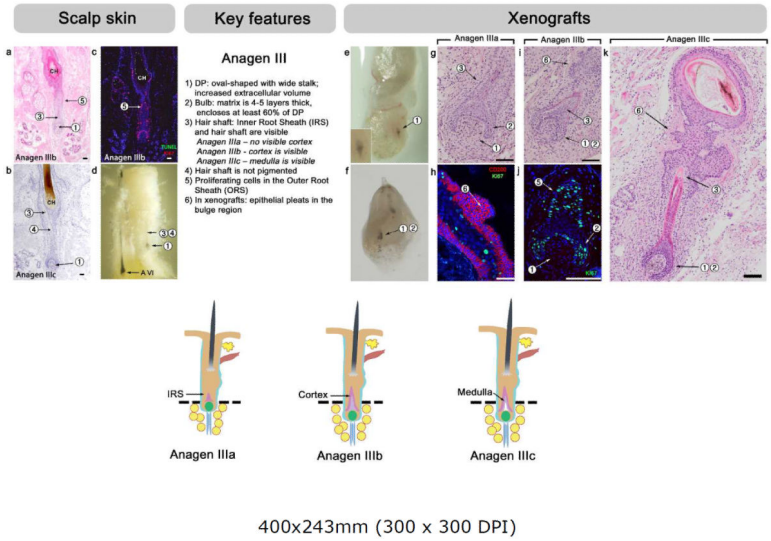

400x243mm (300 x 300 DPI)

Figure 3. Anagen III

Schematic drawings of HFs are provided, and key and auxiliary features are numbered and marked. Key features at this stage are an enlarged, oval-shaped DP (compared to anagen II), the presence of a newly formed, albeit small matrix (4–5 cell layers thick), small, but visible IRS, and a hair shaft that lacks pigmentation. On *in situ*, a newly formed hair bulb enters into the adipose layer. In xenografts, three anagen III sub-stages can be identified on the basis of combined IRS and hair shaft morphology. The bulge region of HFs-XG shows prominent pleats. This stage peaks on post-grafting day 47.

Hosts: SCID mice (panels - f, h, j), nude mice (panels - e, g, i, k).

Scale bars: 100 um.

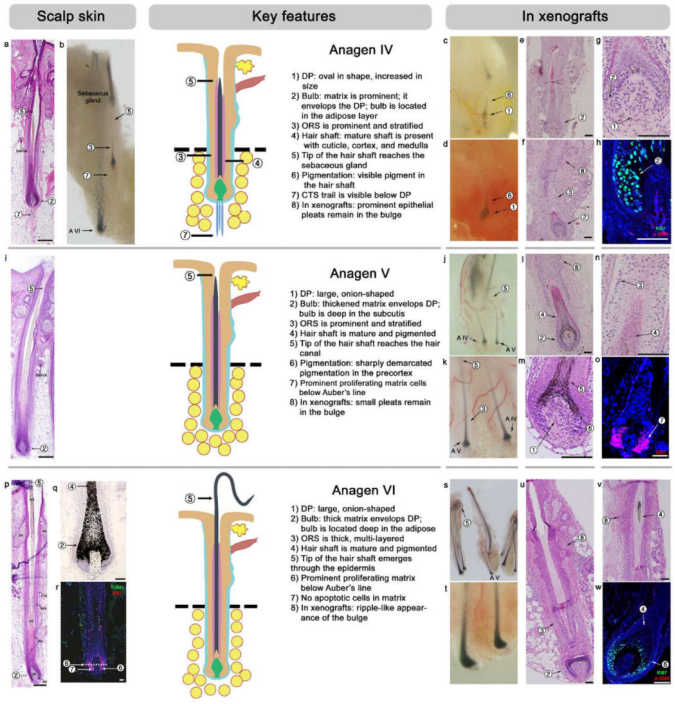

402x421mm (300 x 300 DPI)

Figure 4. Anagen IV, V and VI

For each stage, a schematic drawing is provided, and key and auxiliary features are numbered and marked.

(a–h) Anagen IV in HFs-IS (a, b) and HFs-XG (c-h). Key features at this stage are a prominent matrix, stratified ORS, and a mature hair shaft that reaches the level of the sebaceous gland. On *in situ*, the hair bulb is in the adipose layer, but the connective tissue trail can still be seen (it becomes lost during anagen V). Xenografted anagen IV HFs show prominent pleats in the bulge region and peak on post-grafting day 60.

(i–o) Anagen V in HFs-IS (i) and HFs-XG (j-o). Key features at this stage are a large, onion-shaped DP, significantly increased pigmentation (compared to anagen IV) with sharp demarcation at Auber's line, and a mature hair shaft that reaches the hair canal. On *in situ*, the connective tissue trail disappears (compared to anagen IV). Xenografted anagen V HFs maintain pleats in the bulge region and peak on post-grafting day 63.

(p–w) Anagen VI in HFs-IS (p-r) and HFs-XG (s-w). 90–95% of all HFs-IS are in anagen VI, and all HFs-XG progress to anagen VI by post-grafting day 92. At this stage HFs achieve their maximum size, and the hair shaft tip extends far above the skin surface. There are no apoptotic cells compared to early catagen.

Hosts: SCID mice (panels - e, f, g, m, n, s, t, u, w), nude mice (panels - c, d, h, j, k, l, o, v). Scale bars: 100 um.

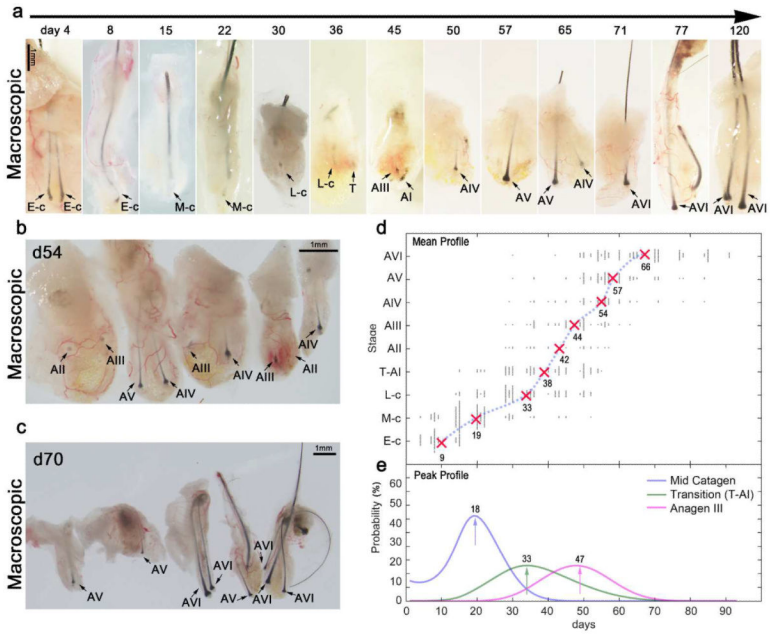

281x230mm (300 x 300 DPI)

Figure 5. Xenograft model optimization

(a) Representative gross morphology of human HFs-XG showing post-grafted hair cycle resetting dynamics: follicles progress through sequential catagen sub-stages, telogen-to-anagen transition stage, and then anagen sub-stages. **(b, c)** Representative images showing hair cycle heterogeneity of HFs-XG at day 54 (b) and 70 (c). **(d)** Comprehensive hair cycle staging of human HFs-XG during the first 90 days (x-axis). Average time point values for each sub-stage (y-axis) are shown with the average regression curve overlaid over the scatter plot of individual HFs stage values (assessed upon biopsy; each dot represents one biopsied HF). **(e)** Statistical analysis of the frequency at which the indicated stage appears (early catagen, telogen-to-anagen I transition, and anagen III). Arrows denote the post-grafting time with the greatest probability of selecting HFs-XG at the indicated stage based on the Naïve Bayes classifier analysis. Further details (for every hair cycle sub-stage) can be found on Supplementary Figure S5.

Hosts: SCID mice (panels – a (days 15, 22, 50, 57, 65) and c), nude mice (panels – a (days 4, 8, 30, 36, 45, 71, 77, 120) and b).

Scale bars: a, b, c – 1mm.